35th AIAA Fluid Dynamics Conference and Exhibit, June 6-9,2005, Toronto,Ontario

Turbomachinery Applications with the Time Spectral Method

Edwin van der Weide*, Arathi K. Gopinath†and Antony Jameson‡
Stanford University, Stanford, CA 94305-4035

This paper presents the Time Spectral Method, which is capable of significantly reducing the CPU requirements for time periodic flows. Here the main focus is turbomachinery computations for which the standard formulation must be adapted to take sector periodicity into account if the problem is solved in the Cartesian frame. Odd-even decoupling is avoided by choosing an odd number of time intervals in a period. Results are presented for the NASA Stage 35 compressor test case and these show that engineering accuracy is obtained with 11 time intervals per blade passing. Especially for high RPM applications, like the Stage 35, the Time Spectral Method leads to a reduction of an order of magnitude in CPU-time compared to a standard second order backward difference time integration scheme.

I. INTRODUCTION

Time dependent periodic calculations find a wide variety of applications including flutter analysis, analysis of flow around helicopter blades in forward flight and rotor-stator combinations in turbomachinery. The last application will be the focus of this paper.

The current industrial practice to solve these problems is to use the mixing plane assumption, i.e. a circumferential averaging is applied at the interface between the rotor and stator grid and consequently a steady state computation is performed for the individual components.[1] Due to the averaging, the result is a rather crude approximation of the rotor-stator interaction and therefore it is desirable to solve the problem in a truly unsteady manner.

The typical way to solve time periodic flow problems is to integrate the governing unsteady equations until the periodic state is reached. The time integration scheme normally used for compressible URANS problems is the implicit second order Backward Difference Formulation (BDF), in which the set of nonlinear equations for the new state is solved using the dual time stepping approach in combination with standard convergence acceleration techniques such as multigrid and local time stepping.[2] Typically 50 to 100 multigrid cycles are needed for every time step for an accurate solution of the URANS equations for turbomachinery problems.

It normally takes 5-10 "particle flow-through times" before the periodic state is (approximately) reached even when a restart is made from the mixing plane solution. For high-RPM machines this corresponds to a couple of revolutions, see section III. Combined with the 50 to 100 multigrid cycles per time step, at least 50 time steps per blade passing and 40-150 blades per row, this leads to the order of 500,000 multigrid cycles and thus to excessive wall clock times even on the largest supercomputers available.

Following the direction suggested by Hall et.al.[3,4,5] the Time Spectral Method is presented to solve time-periodic unsteady problems. The Fourier method is used for time discretization, leading to spectral accuracy. When the formulae are transformed back to the physical domain, the time derivative appears as a high-order central difference formula coupling all the time levels in the period. As for the BDF method, dual time stepping and the standard convergence acceleration techniques are used as an iterative method to obtain the solution. The advantage of solving the equations directly in the time domain rather than in the

*Research Associate, AIAA Member
†Doctoral Candidate, AIAA Student Member
‡Thomas V. Jones Professor of Engineering, Department of Aeronautics and Astronautics, AIAA Member

frequency domain, is that the method can be implemented relatively easily in an existing CFD code, whereas when the problem is solved in the frequency domain, a completely new code must be developed involving complex arithmetic.

Firstly the general formulation is described and the problem of odd-even decoupling is discussed. Then the general formulation is extended to problems with sector periodicity where the periodicity is less than the entire revolution. Results will be shown for the NASA Stage 35 compressor and conclusions and future work will conclude this paper.

II. MATHEMATICAL FORMULATION

A. Formulation of the Time Spectral Method

The Navier-Stokes equations in integral form are given by

$$\int_{\Omega} \frac{\partial w}{\partial t}\, dV + \oint_{\partial\Omega} \vec{F} \cdot \vec{n}\, ds = 0. \tag{1}$$

where w are the conservative variables and $\vec{F}$ is the corresponding flux vector, which includes the effect of a moving control volume. The semi-discrete form of equation (1) is obtained by discretizing only the spatial part, which can be expressed as

$$V\frac{\partial w}{\partial t} + R(w) = 0. \tag{2}$$

For convenience sake the control volume is assumed to be constant in time, i.e. only rigid body motions are considered. However the analysis below can be extended to deforming meshes if Vw is assumed to vary in time rather than w.

State-of-the-art time accurate solvers do not take advantage of the periodic nature of the flow. If this information is taken into account, a Fourier representation in time can make it possible to achieve spectral accuracy. Suppose the time period is given by T and is divided into N time steps, and $\Delta t = T/N$. If N is even the discrete fourier transform of w is then given by

$$\hat{w}_k = \frac{1}{N}\sum_{n=0}^{N-1} w^n e^{-ikn\Delta t} \tag{3}$$

and its inverse transform by

$$w^n = \sum_{k=-\frac{N}{2}}^{\frac{N}{2}-1} \hat{w}_k e^{ikn\Delta t}. \tag{4}$$

If the operator D_t is defined as the spectral time derivative for the unsteady term, equation (2) can be written as

$$VD_t w^n + R(w^n) = 0. \tag{5}$$

McMullen et.al.[6,7] solved the time accurate equations (5) by transforming them into the frequency domain. Alternatively, the Time Spectral Method proposes to solve the governing equations in the time-domain, considerably gaining on the computational time required, because the transformation back and forth to the frequency domain is avoided.

From equation (4), the time discretization operator D_t^{even} can be written as

$$D_t^{even} w^n = \frac{2\pi}{T}\sum_{k=-\frac{N}{2}}^{\frac{N}{2}-1} ik\hat{w}_k e^{ikn\Delta t}.$$

This summation, involving the fourier modes $\hat{w}_k$, can be rewritten in terms of the variables w in the time domain as

$$D_t^{even} w^n = \frac{2\pi}{T}\sum_{m=-\frac{N}{2}+1}^{\frac{N}{2}-1} d_m^{even} w^{n+m}, \tag{6}$$

where the coefficients d_m^{even} are given by, see also[8]

$$d_m^{even} = \begin{cases} \frac{1}{2}(-1)^{m+1} cot(\frac{\pi m}{N}) & : \quad m \neq 0 \\ 0 & : \quad m = 0 \end{cases} \tag{7}$$

If N is odd a very similar derivation can be performed, which results in the following formulation for the time derivative

$$D_t^{odd} w^n = \frac{2\pi}{T} \sum_{m=\frac{1-N}{2}}^{\frac{N-1}{2}} d_m^{odd} w^{n+m}, \tag{8}$$

with the coefficients

$$d_m^{odd} = \begin{cases} \frac{1}{2}(-1)^{m+1} cosec(\frac{\pi m}{N}) & : \quad m \neq 0 \\ 0 & : \quad m = 0 \end{cases} \tag{9}$$

Note that $d_{-m} = -d_m$ for both the even and odd number of time intervals, see equations (7) and (9). Hence the operator D_t is a central difference operator connecting all the time levels, yielding an integrated space-time formulation which requires the simultaneous solution of the equations for all time levels.

Completely equivalent to the dual time stepping technique for the BDF, a pseudo-time t^* can be introduced to time march the equations (5) to a periodic state

$$V \frac{\partial w^n}{\partial t^*} + V D_t w^n + R(w^n) = 0. \tag{10}$$

B. Stability

The addition of the time derivative term $D_t w$ in equation (10) must be taken into account in the definition of the pseudo-time step Δt^*, in comparison with solving a steady-state problem.

The frequency domain method transforms equation (5) into the frequency domain and solves it using a similar pseudo-time stepping approach,

$$V \frac{\partial \hat{w}_k}{\partial t_k^*} + V \frac{2\pi}{T} ik \hat{w}_k + \hat{R}_k = 0, \tag{11}$$

where t_k^* is the pseudo-time for wave number k. Note that the orthogonality of the Fourier coefficients ensures that the equations corresponding to each wave number are decoupled. From a stability analysis for the frequency domain method, the pseudo-time step Δt_k^* can be estimated to be

$$\Delta t_k^* = \frac{CFL * V}{||\lambda|| + k' * V}, \tag{12}$$

where V is the volume of a cell, $||\lambda||$ is the spectral radius of the flux Jacobian of the spatial part of the equations and $k' = k * \frac{2\pi}{T}$. I.e. an additional term based on the wave number is added to the denominator of equation (12) compared to the standard time step definition for a steady-state problem. Hence the pseudo-time step is based on the wave number for each frequency and thus different for every frequency.

To estimate a frequency-based pseudo-time step limit for the Time Spectral Method that is solved in the time domain, consider the inverse fourier transform of equation (11) back to the time domain,

$$F^{-1}(V \frac{\Delta \hat{w}_k}{\Delta t_k^*} + V \frac{2\pi}{T} ik \hat{w}_k + \hat{R}_k) = 0. \tag{13}$$

or

$$F^{-1}(V \frac{\Delta \hat{w}_k}{\Delta t_k^*}) + V \frac{\partial w}{\partial t} + R(w) = 0. \tag{14}$$

This inverse fourier transform operation with different time steps Δt_k^* in the frequency domain, will transform to a matrix time step in the time domain coupling all the time levels. As the spectral radius varies from cell to cell, this matrix will have to be inverted in each cell and at every stage of the multigrid cycle, which makes this approach rather costly.

Alternatively, it is possible to use a constant time-step in the frequency domain corresponding to the smallest wave number, i.e. the most restrictive time-step. Then,

$$\Delta t_k^* = \frac{CFL * V}{||\lambda|| + k' * V} \tag{15}$$

where

$$k' = \begin{cases} \frac{N}{2} * \frac{2\pi}{T} & : \quad N \text{ is even} \\ \frac{N-1}{2} * \frac{2\pi}{T} & : \quad N \text{ is odd} \end{cases} \tag{16}$$

On transforming back to the time domain, the time-step for each time instance is constant and retains the form of Δt_k^* since it is independent of the wave-numbers. The choice of time-step (16) is rather restrictive, especially when the number of time intervals increases. However it considerably reduces the computational cost involved in inverting a matrix several times.

C. Odd-even decoupling

Equations (6) and (8) can be written as a matrix vector multiplication

$$D_t w = DW, \tag{17}$$

where $W = (w^1, w^2, \cdots, w^N)^T$ and the matrix D is given by

$$D^{even} = \begin{pmatrix} 0 & d_1^{even} & \cdots & d_{\frac{N}{2}-1}^{even} & 0 & -d_{\frac{N}{2}-1}^{even} & \cdots & -d_1^{even} \\ -d_1^{even} & 0 & d_1^{even} & d_2^{even} & \cdots & 0 & \cdots & -d_2^{even} \\ \vdots & \vdots & \vdots & \vdots & \vdots & \vdots & \vdots & \vdots \\ d_1^{even} & d_2^{even} & \cdots & 0 & \cdots & -d_2^{even} & -d_1^{even} & 0 \end{pmatrix} \tag{18}$$

for an even number of time intervals and by

$$D^{odd} = \begin{pmatrix} 0 & d_1^{odd} & \cdots & d_{\frac{N-1}{2}}^{odd} & -d_{\frac{N-1}{2}}^{odd} & \cdots & -d_1^{odd} \\ -d_1^{odd} & 0 & d_1^{odd} & d_2^{odd} & \cdots & \cdots & -d_2^{odd} \\ \vdots & \vdots & \vdots & \vdots & \vdots & \vdots & \vdots \\ d_1^{odd} & d_2^{odd} & \cdots & \cdots & -d_2^{odd} & -d_1^{odd} & 0 \end{pmatrix} \tag{19}$$

for an odd number of time intervals. From equation (18) it is clear that every row of D^{even} contains two zeros, while the rows of D^{odd} only have one. As a consequence D^{even} has two zero eigenvalues with eigenvectors $e_1 = (1, 1, \cdots, 1)^T$ and $e_2 = (1, 0, 1, 0, \cdots, 1, 0)^T$. Eigenvector e_1 corresponds to a zero time derivative for a constant solution, a property of a consistent scheme. However also eigenvector e_2 results in a discrete zero time-derivative, while e_2 clearly corresponds to an odd-even decoupled solution, i.e. this mode is not damped by D^{even}.

D^{odd} on the other hand only has one zero eigenvalue with corresponding eigenvector $e_1 = (1, 1, \cdots, 1)^T$. Consequently the odd-even decoupled solution does not lead to a discrete zero time-derivative for D^{odd}.

It was found that for cases where the time derivative is relatively small both D^{even} and D^{odd} are stable, e.g. pitching airfoils and wings.[9] However for problems where the time derivative is important, e.g. high RPM turbomachinery problems, the odd-even decoupling introduces instabilities, which lead to failure of the algorithm using an even number of time intervals. Consequently for those cases only an odd number of time intervals can be used.

D. Sector periodicity

In turbomachinery problems often only a part of the entire wheel is simulated to keep the problem size within acceptable limits. Consequently sector periodic boundary conditions must be used to obtain a well-posed problem. If a cylindrical coordinate system is chosen to solve the problem, all the formulae presented so far can be used without modification. However in this work the Cartesian formulation of the governing

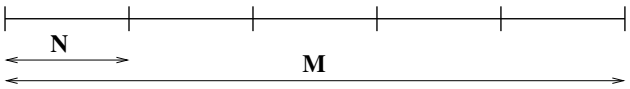

Figure 1. Sector periodic subproblem with N time steps and entire wheel with M time steps, where $M = PN$, P is an integer; for the case shown $P = 5$.

equations (2) is solved, such that the flow solver can be used for all kind of problems and is not limited to turbomachinery only. If the Time Spectral Method is then used to discretize the time derivatives for such a sector periodic problem, equations (6), (7), (8) and (9) are not valid anymore, because the momentum vectors are rotated between periodic boundaries. Below is shown that it is still possible to use the Time Spectral Method on only a part of the wheel if the coefficients of the time derivatives for vector quantities are modified.

Suppose the entire wheel is modeled using M time steps and the sector periodic subproblem with N time steps, where $M = PN$, see figure 1. Here P is the number of periodic sections present in the entire wheel.

For the entire wheel the solution is certainly periodic, i.e.

$$w^{j+M} = w^j, \tag{20}$$

where j is an arbitrary time index. Relation (20) holds for both scalar and vector quantities and therefore equations (6), (7), (8) and (9) are valid when the entire wheel is considered.

Splitting the sum in equation (6) in a part with positive and in a part with negative indices and introducing the superscript M to indicate that these coefficients are valid for the time interval T_M, the time to complete one revolution, results in

$$D_t^{even} w^l = \frac{2\pi}{T_M} \left\{ \sum_{m=1-\frac{M}{2}}^{-1} d_m^M w^{l+m} + \sum_{m=1}^{\frac{M}{2}-1} d_m^M w^{l+m} \right\}. \tag{21}$$

For equation (8) this procedure leads to

$$D_t^{odd} w^l = \frac{2\pi}{T_M} \left\{ \sum_{m=\frac{1-M}{2}}^{-1} d_m^M w^{l+m} + \sum_{m=1}^{\frac{M-1}{2}} d_m^M w^{l+m} \right\}. \tag{22}$$

In equations (21) and (22) the superscripts *even* and *odd* are omitted from d_m^M for clarity reasons.

Using the periodicity of the solution, equation (20), and the periodicity of the coefficients d_m^M, $d_m^M = d_{m+M}^M$, the running index in the first sum in equations (21) and (22) can be incremented by M. This results in one formulation for both even and odd number of time intervals. The time derivative in point l is then given by

$$D_t w^l = \frac{2\pi}{T_M} \sum_{m=1}^{M-1} d_m^M w^{l+m}, \tag{23}$$

where for an even number of time intervals use is made of $d_{\frac{M}{2}}^M = 0$. An alternative way of writing equation (23) is

$$D_t w^l = \frac{2\pi}{T_M} \left[\sum_{p=0}^{P-1} \sum_{n=1}^{N-1} d_{n+pN}^M w^{l+n+pN} \right] + \frac{2\pi}{T_M} \left[\sum_{p=1}^{P-1} d_{pN}^M w^{l+pN} \right]. \tag{24}$$

The second sum of equation (24) can be incorporated in the double sum if the index n starts at 0 instead of 1. However, it is kept separate, because this term vanishes for scalar quantities if sector periodicity is taken into account.

Now assume that w is a vector and furthermore assume that point l belongs to a rotating part of the grid, i.e. point l moves in time. Then the following relation holds

$$w^{j+pN} = R^p w^j, \tag{25}$$

where R is the rotation matrix between the periodic sections. Note that the superscript p in R^p is an actual power, i.e. $R^p = R * R * \ldots * R$. Combining equations (24) and (25) results in

$$D_t w^l = \frac{2\pi}{T_M} \left[\sum_{p=0}^{P-1} \sum_{n=1}^{N-1} d^M_{n+pN} R^p w^{l+n} \right] + \frac{2\pi}{T_M} \left[\sum_{p=1}^{P-1} d^M_{pN} R^p w^l \right]. \tag{26}$$

It is clear that the superscript of the solution w does not depend anymore on the summation index p. Therefore the matrices d^N_n and e^N can be defined as

$$\begin{aligned} d^N_n &\overset{def}{=} \frac{1}{P} \sum_{p=0}^{P-1} d^M_{n+pN} R^p \\ e^N &\overset{def}{=} \frac{1}{P} \sum_{p=1}^{P-1} d^M_{pN} R^p \end{aligned} \tag{27}$$

Combining equations (26) and (27) and making use of the fact that $T_M = PT_N$, the time derivative for point l becomes

$$D_t w^l = \frac{2\pi}{T_N} \sum_{n=1}^{N-1} d^N_n w^{l+n} + \frac{2\pi}{T_N} e^N w^l. \tag{28}$$

A few things can be noted. First $d^N_n \neq d^N_{N-n}$, i.e. the time derivative is not a true central difference anymore, second the time derivative in point l now depends on the state in point l via e^N and third the derivative of e.g. the x-component of the vector depends on the y and z components.

For completeness consider the scalar (or non-rotating) case, i.e. $R = I$. From the definition of d^M_m, equations (7) and (9), and e^N, equation (27) it is clear that for the scalar case $e^N = 0$. The definition of d^N_n simplifies to

$$\begin{aligned} \left(d^N_n\right)^{\text{scal}} &= \frac{1}{P} \sum_{p=0}^{P-1} d^M_{n+pN} \\ &= \begin{cases} \dfrac{1}{P} \displaystyle\sum_{p=0}^{P-1} \frac{1}{2} (-1)^{n+pN+1} \, cot\left(\frac{\pi(n+pN)}{M}\right) & M \text{ is even} \\ \dfrac{1}{P} \displaystyle\sum_{p=0}^{P-1} \frac{1}{2} (-1)^{n+pN+1} \, cosec\left(\frac{\pi(n+pN)}{M}\right) & M \text{ is odd} \end{cases} \end{aligned} \tag{29}$$

The definition of d^N_n in equation (29) should be identical to the expression obtained by applying equation (23) directly to the period N, i.e.

$$\left(d^N_n\right)^{\text{scal}} = \begin{cases} \dfrac{1}{2} (-1)^n \, cot\left(\dfrac{\pi n}{N}\right) & N \text{ is even} \\ \dfrac{1}{2} (-1)^n \, cosec\left(\dfrac{\pi n}{N}\right) & N \text{ is odd} \end{cases}. \tag{30}$$

It can be proved that this is indeed the case.

III. RESULTS

Gopinath et.al.[9] validated the Time Spectral Method for pitching airfoils and wings and showed that with only 4 time intervals per pitching period engineering accuracy is obtained for these type of problems.

In this work the method is applied to turbomachinery problems and results will be shown for the high RPM NASA Stage 35 compressor. As the primary focus of this paper is verification of the Time Spectral Method for turbomachinery applications rather than validation, the geometry has been modified such that the blade counts are identical and the computations can be done using only one blade passage. This simplification leads to a considerable saving in the CPU-requirements while still a comparison can be made with the standard BDF technique.

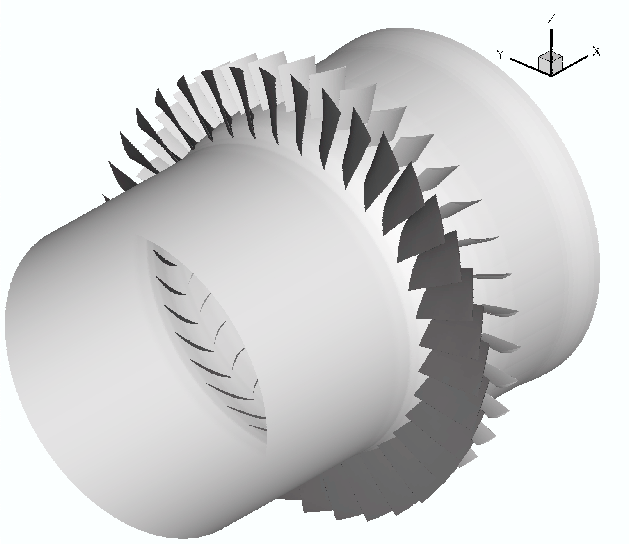

Figure 2. 1-1 scaled geometry for the NASA Stage 35 compressor. Both the rotor and stator contain 36 blades.

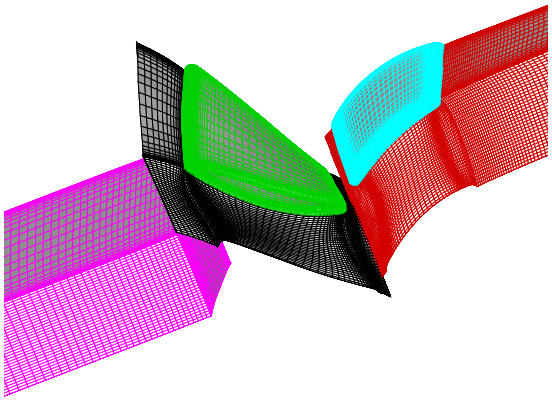

Figure 3. Multiblock structured mesh for the 1-1 scaled Stage 35 compressor. The volume grid contains 773,184.

The flow solver used in this work is TFLO2000,[10] a compressible multiblock RANS code which has been developed recently at Stanford under the scope of the Department of Energy's (DoE) ASC (Advanced Simulation and Computing Program).[11] TFLO2000 uses a cell-centered finite volume formulation in which the inviscid fluxes are either calculated with a central difference scheme augmented with artificial dissipation[12] or an upwind scheme in combination with Roe's approximate Riemann solver.[13] The viscous fluxes are computed using a central discretization. The convergence is accelerated using a standard geometrical multigrid algorithm in combination with an explicit multi-stage Runge-Kutta scheme. Although it is possible to apply residual averaging it was found that for the type of problems considered in this work this did not lead to a significant gain in efficiency.

TFLO2000 incorporates a number of turbulence models, possibly in combination with wall functions.[14] The quasi-linear form of the additional transport equations are solved in a decoupled manner from the mean flow equations using a DD-ADI scheme.[15] The advection part of the these equations are discretized using either a first or second order upwind discretization while a central discretization is used for the viscous terms. No multigrid is applied to the turbulence equations.

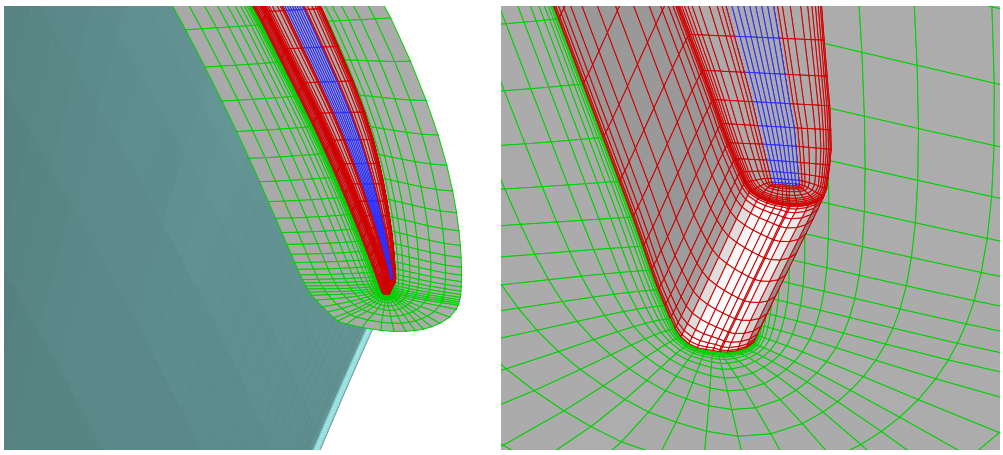

Figure 4. Block topology in the tip gap region of the rotor of the Stage 35

.

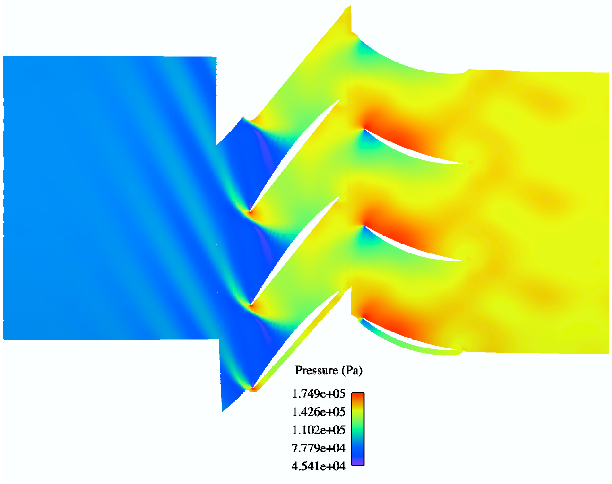

Figure 5. Instantaneous pressure distribution in a radial plane halfway the hub and the case for the 1-1 scaled NASA Stage35 compressor.

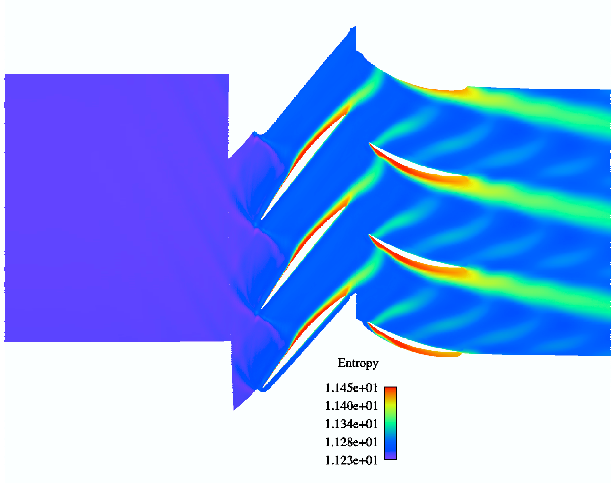

Figure 6. Instantaneous entropy distribution in a radial plane halfway the hub and the case for the 1-1 scaled NASA Stage35 compressor.

1. NASA Stage 35 compressor

The NASA Stage 35 test case[16] is a low aspect ratio transonic compressor. The rotor contains 36 blades and the stator has 46 blades, where the rotor rotates at 17,119 RPM. The stator has been scaled to 36 blades, such that a 1-1 configuration is obtained, see figure 2. Due to the high rotation rate and the consequently large CPU times for the BDF method a rather coarse grid is used, see figure 3. It consists of 7 blocks and the volume grid contains 773,184 cells. The spacing normal to the viscous boundaries is such that an y^+-value of $O(1)$ is obtained. Figure 4 shows the block topology used in the tip gap region of the rotor. This topology avoids singular lines, which is beneficial for both the stability of the code and the quality of the solution.

As an inlet and outlet block are present, figure 3, uniform boundary conditions can be used. At the inlet the flow is assumed to be axial with a total pressure of 101.3 kPa and a total temperature of 288 K. At the outlet a static pressure of 101.3 kPa has been prescribed.

Scalar artificial dissipation[12] has been used for the inviscid part of the mean flow equations; fully turbulent flow has been assumed where the eddy-viscosity is modeled using the standard $k-\omega$ model.[17] Only a 2W multigrid cycle is used to accelerate the convergence due to restrictions imposed by the block dimensions.

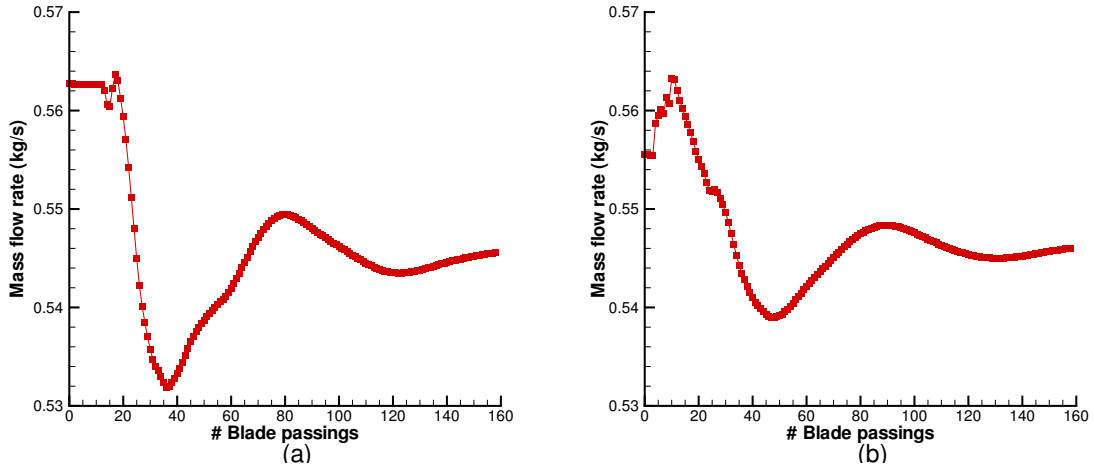

Figure 7. Mass flow rate for the 1-1 scaled Stage35 compressor for the BDF computation. The values are given every 50 time steps, which is the blade passing time. (a) Domain inlet, (b) Domain outlet.

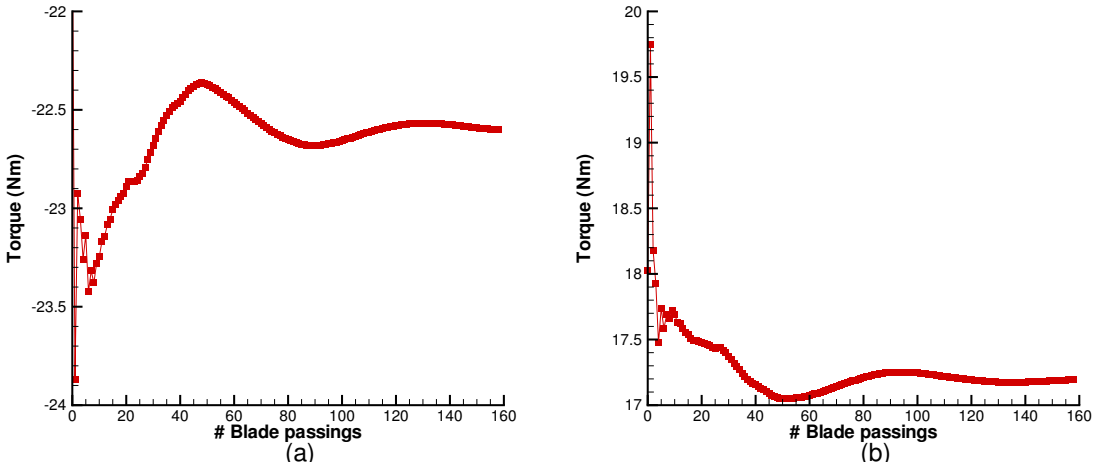

Figure 8. Torque on the blades for the 1-1 scaled Stage35 for the BDF computation. The values are given every 50 time steps, which is the blade passing time. (a) Rotor, (b) stator.

The mixing plane technique is used to create an initial solution for the BDF method. A blade passing has been resolved with 50 time steps and 50 multigrid cycles were used to solve the nonlinear system for every time step. The instantaneous pressure and entropy fields for the periodically converged solution in a radial grid plane halfway between the hub and the case are depicted in figures 5 and 6. Especially the latter clearly shows the impinging wakes of the rotor on the stator; an effect that cannot be captured by the mixing plane assumption. The rotation rate is such that the flow is supersonic in the leading edge region of the rotor. Consequently a detached shock wave is present which impinges on the neighboring blade on one side and travels upstream towards the inlet on the other side.

Figures 7 and 8 show the massflow and torque on the blades every 50 time steps until the periodic state is reached; 50 time steps is the time required for one blade passing, which is the periodic time for this case. It is clear that even after 8,000 time steps, i.e. almost 4.5 revolutions the periodic state has not fully been reached; 8,000 time steps correspond to 400,000 multigrid cycles.

The Time Spectral Method has been used for this case in combination with 3, 5, 7, 9, 11 and 13 time

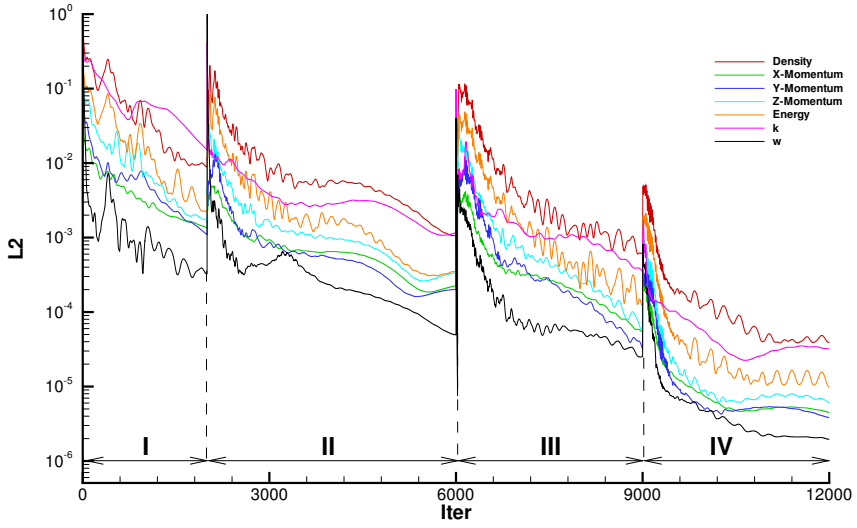

Figure 9. Convergence history for the Time Spectral Method for the 1-1 scaled Stage 35. Part I: Mixing plane solution, Part II: 3 time intervals, Part III: 9 time intervals, Part IV: 11 time intervals

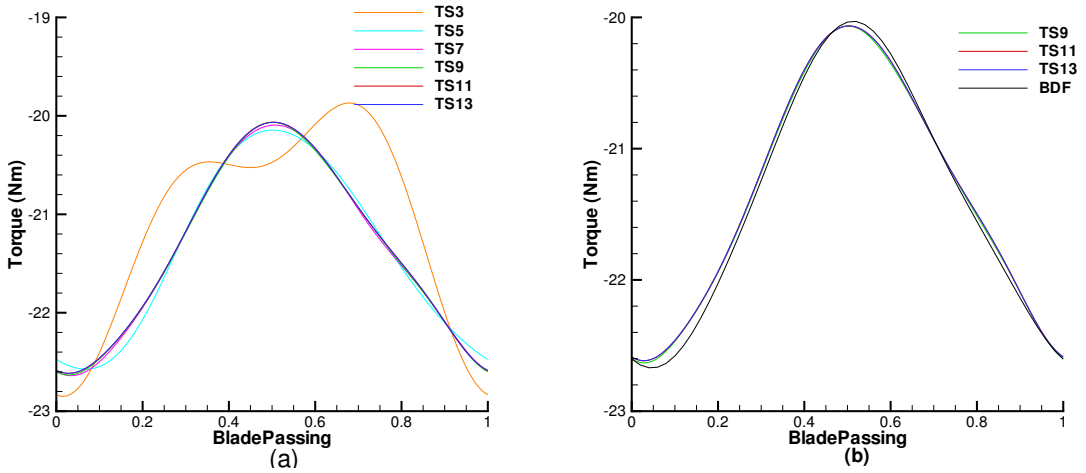

Figure 10. Torque on the rotor blade for the 1-1 scaled Stage35 compressor during a blade passing; (a) time convergence for the time spectral method, (b) comparison between the time spectral solutions and BDF solution with 50 time steps per blade passing.

intervals per blade passing. The solutions have been computed using the following strategy. First an initial solution has been obtained for the 3 time interval case using the mixing plane technique. Then the converged solution of the 3 time interval case was used as the starting solution for 5, 7 and 9 time intervals (using spectral interpolation). Finally the solution of the 9 time interval case was used to start the computation with 11 and 13 time intervals. The entire convergence history for 11 time intervals is shown in figure 9. Due to the fact that only a 2 level W-cycle could be used and the conservative estimate from equation (16), relatively many iterations are needed to obtain a converged solution. For 11 time intervals this corresponds to 70,000 equivalent multigrid cycles of the BDF method.

Figures 10 and 11 show the periodic solutions of the torque on the rotor and stator blades for the Time Spectral method during a blade passing as well as a comparison with the second order BDF method. It is clear that the torque on the rotor blade is predicted quite well with just 5 time intervals and can be considered time converged with only 7 time intervals per blade passing, despite the presence of the strong shock wave in the rotor blade passage. The reason is that the shock is steady in the rotating frame and this effect can be captured by only one harmonic, i.e. 3 time intervals. The effect of the stator on the rotor is relatively small and can be captured almost entirely by the second harmonic. The agreement between the time spectral solutions and the second order BDF method is excellent; the small discrepancies can be explained by the fact that the BDF solution has not fully reached the periodic state and may not be time converged, see later.

For the stator the situation is different. As can be seen in figure 6 the wakes of previous rotors are clearly visible in the blade passage of the stator and therefore the effect of previous rotor blades on the stator is significant. Due to the velocity difference between the suction and pressure side of the stator blade, indicated by the rotation of the rotor wakes in the blade passage, higher harmonic frequencies are present. As a result more time intervals are needed to obtain an accurate prediction. Figure 11 shows that for 11 time intervals per blade passing the solution can be considered time converged.

The comparison between the time spectral solutions and the BDF solution with 50 time steps per blade passing, figure 11, shows a rather dissipative behavior for the latter. This is an indication that, due to the more complex unsteady flow features in the stator passage, 50 time steps per blade passing for the BDF is not enough to capture all the phenomena accurately.

The conclusion for this case is that the Time Spectral Method leads to a saving of a factor of 6 in CPU time compared to the standard BDF method, 70,000 vs. 400,000 multigrid cycles, while the quality of the solution is better. To obtain the same resolution in time the number of time steps per blade passing should be increased for the BDF method and then the reduction in CPU time for the Time Spectral Method will be one order of magnitude.

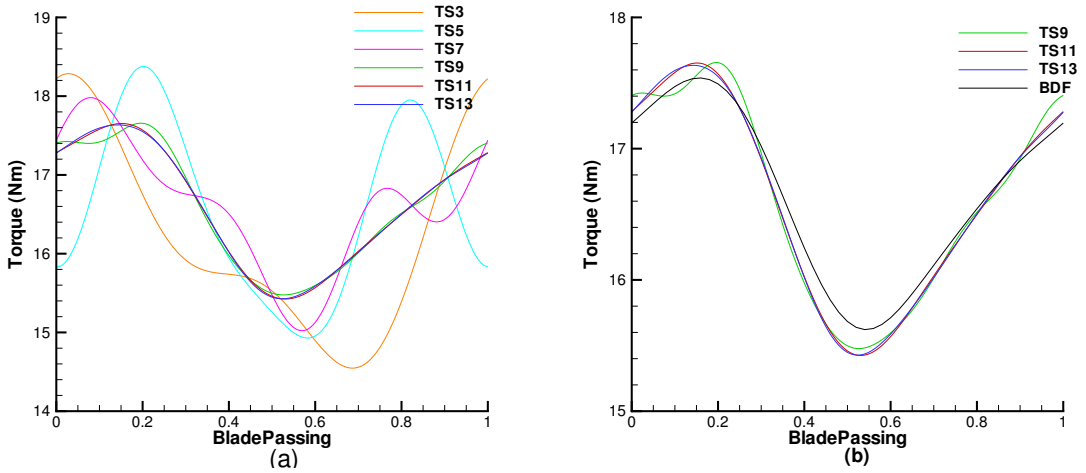

Figure 11. Torque on the stator blade for the 1-1 scaled Stage35 compressor during a blade passing; (a) time convergence for the time spectral method, (b) comparison between the time spectral solutions and BDF solution with 50 time steps per blade passing.

IV. CONCLUSIONS AND FUTURE WORK

The formulation for the Time Spectral Method has been presented for time periodic flows as well as a correction needed for the Cartesian formulation to treat sector periodicity. Numerical results for the 1-1 scaled NASA Stage 35 compressor show that the Time Spectral Method is able to achieve at least the same accuracy as more standard time integration schemes, e.g. the second order BDF, with a relatively small number of time intervals. Especially for high RPM problems, like the Stage 35, this leads to an order of magnitude reduction of the CPU-requirements compared to the BDF formulation.

It is desirable that the true geometry is computed rather than the 1-1 scaled geometries. In principle it is possible to apply the Time Spectral Method to the true geometry, but the requirement of $O(10)$ time intervals per blade passing will then lead to an unfavorable comparison compared to BDF types of methods. This is also because the implementation is very memory intensive, since the solutions of all time intervals need to be stored.

A much more interesting approach is to use the Time Spectral Method in combination with the phase lag assumption.[18,19] This assumption allows a time accurate computation with only one blade passage, even if the periodic angles of the different blade rows do not match. The entire machinery presented in this paper can then be used again, albeit in slightly modified form, because interpolation in time must be applied for the general case on the sliding mesh interface between the rotor and stator as well as on the periodic boundaries. Compared to full wheel computations with a BDF type scheme, the CPU requirements are orders of magnitude less, while still the main unsteady information of the flow field is obtained.

Of course the phase lag assumption results in a reduced order model for the time derivative, which may not be suited for a high fidelity simulation. However, the Time Spectral Method can then still be used to provide a very good initial guess for the standard BDF scheme such that a high quality periodic solution can be obtained much faster.

V. ACKNOWLEDGMENT

This work has benefited from the generous support of the Department of Energy under contract number LLNL B341491 as part of the Advanced Simulation and Computing Program (ASC) program at Stanford University.

References

[1]J.D. Denton and U.K. Singh. Time marching methods for turbomachinery flows. In *VKI LS 1979-07*, 1979.

[2]A. Jameson. Time dependent calculations using multigrid, with applications to unsteady flows past airfoils and wings. (91-1596), June 1998.

[3]K.C. Hall, J.P. Thomas, and W.S. Clark. Computation of unsteady nonlinear flows in cascades using a harmonic balance technique. *AIAA Journal*, 40(5):879–886, May 2002.

[4]K.C. Hall and K. Ekici. Multistage coupling for unsteady flows in turbomachinery. *AIAA Journal*, 43(3):624–632, March 2005.

[5]K.C. Hall, R.E. Kielb, K. Ekici, and J.P. Thomas. Recent advancements in turbomachinery aeroelastic design analysis. *AIAA paper 05-0014*, AIAA 43rd Aerospace Sciences Meeting and Exhibit, Reno, NV, January 2005.

[6]M. McMullen, A. Jameson, and J.J. Alonso. Acceleration of convergence to a periodic steady state in turbomachinery flows. *AIAA paper 01-0152*, AIAA 39th Aerospace Sciences Meeting, Reno, NV, January 2001.

[7]M. McMullen, A. Jameson, and J.J. Alonso. Application of a non-linear frequency domain solver to the euler and navier-stokes equations. *AIAA paper 02-0120*, AIAA 40th Aerospace Sciences Meeting and Exhibit, Reno, NV, January 2002.

[8]A.Quarteroni C.Canuto, M.Y.Hussaini and T.A. Zang. *Spectral Methods in Fluid Dynamics; Springer Series in Computational Physics*. Springer Verlag, 1988.

[9]A. Gopinath and A. Jameson. Time spectral method for periodic unsteady computations over two- and three- dimensional bodies. *AIAA paper 05-1220*, AIAA 43rd Aerospace Sciences Meeting and Exhibit, Reno, NV, January 2005.

[10]Annual technical report. Center for Integrated Turbulence Simulations, Stanford University, CA, 2003.

[11]Annual asc report. http://cits.stanford.edu.

[12]A. Jameson, W. Schmidt, and E. Turkel. Numerical solution of the euler equations by finite volume methods using runge kutta time stepping schemes. 1981. AIAA paper 81-1259.

[13]P. Roe. Fluctuations and signals - a framework for numerical evolution problems. In *Numerical Methods for Fluid Dynamics*. Academic Press, 1982.

[14]G. Medic, G. Kalitzin, G. Iaccarino, and E. van der Weide. Adaptive wall functions with applications. *AIAA Journal*, 2005. Submitted for publication.

[15]G. Kalitzin. An efficient and robust algorithm for the solution of the v2-f turbulence model with application to turbomachinery flow. In *WEHSFF 2002 Conference*, Marseille, April 2002.

[16]L. Reed and R.D. Moore. Performance of single-stage axial-flow transonic compressor with rotor and stator aspect ratios of 1.19 and 1.26, and with design pressure ratio of 1.82. Technical report, NASA, 1978. TP 1338.

[17]D.C. Wilcox. Reassesment of the scale-determining equation for advanced turbulence models. *AIAA-Journal*, 26(11):1299–1310, 1988.

[18]X. Wang and J. Chen. A post-processor to render turbomachinery flows using phase-lag simulations. *AIAA paper 04-615*, AIAA 42nd Aerospace Sciences Meeting and Exhibit, Reno, NV, January 2004.

[19]J.P. Chen and J.W. Barter. Comparison pf time-accurate calculations fpr the unsteady interaction in turbomachinery stage. *AIAA paper 98-3292*, July 1998.